Stability of Magnetic Domains With Notches in Permalloy Nanowires

Junyeon Kim[1], Myung-Hwa Jung[2], and Sug-Bong Choe[1]

[1]Center for Subwavelength Optics and School of Physics and Astronomy, Seoul National University, Seoul 151-742, Republic of Korea
[2]Department of Physics, Sogang University, Seoul 121-742, Republic of Korea

Thermal stability of magnetic domains in ferromagnetic Permalloy nanowires is investigated by means of micromagnetic calculation with finite temperature. The magnetic domains, initially placed between two domain walls pinned at either artificial notches or edge roughness, are examined to be collapsed or not with thermal fluctuation. The stable domain size is revealed to be linearly dependent on the wire width, with different proportionality for different domain wall types—either transverse or vortex wall, irrespective to the wall alignment—either parallel or antiparallel to each other. The vortex walls provide regular stable domain size insensitive to the wire edge roughness, whereas the stability with the transverse walls is much influenced.

***Index Terms*—Magnetic domains, micromagnetism, thermal stability.**

I. INTRODUCTION

IN magnetic memory and/or logic devices based on ferromagnetic nanowires [1], [2], the data are stored in the form of the magnetic domains and thus, the storage density is determined by the minimum size of stable domains [3]. In ideal straight nanowires without edge roughness, no stable domains are expected since there is no pinning potential for the domain walls along the wires. However, the natural edge roughness as well as artificial notch induces the domain wall pinning effect [4]–[6] and consequently, the stability of the magnetic domains is attained. Here, we examine the stability of the magnetic domains in ferromagnetic Permalloy nanowires. For this study, micromagnetic calculation with consideration of the finite temperature is adopted to check the collapse of domains with thermal fluctuation. The magnetic domains with various lengths are initially placed between two domain walls pinned at either natural edge roughness or artificial notches. Four configurations are then tested with two different domain-wall types either the transverse or vortex walls, aligned either parallel or antiparallel to each other.

II. CALCULATION METHOD

Fig. 1 shows two test structures of (a) the case I and (b) the case II, respectively. In the case I, the nanowire has no edge roughness except two artificial notches separated by the distance l, whereas in the case II, in addition to the same artificial notches as in the case I, the nanowire has periodic edge roughness. The edge roughness consists of series of triangular vacancies with 30-nm period and 10-nm depth, mimicking typical roughness produced in the nanofabrication. For direct comparison, the artificial notches are also given by the same structure with 10-nm deep vacancy. We have chosen a relatively smaller notch size, to test the worst limit of the domain wall stability. The magnetostatic dipolar field from the wire ends is artificially removed

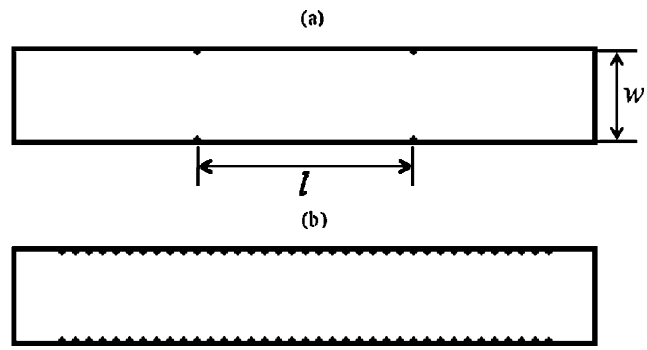

Fig. 1. Nanowire structures under examination for (a) the case I of ideal wires with two artificial notches and (b) the case II of the wires with edge roughness.

by preliminary calculation of the magnetostatic field at the saturated state. To remove the magnetostatic dipolar field from the artificial wire ends, we first calculate the magnetostatic field distribution at the saturated state of 10-times longer nanowire and then, the capture the magnetostatic field distribution from each wire end. By adding the calculated magnetostatic field into the simulation as constant external magnetic field, the magnetostatic field at the wire ends is compensated (i.e., removed). 5-nm-thick wires with various widths w ranging from 60 to 200 nm with 20 nm step are examined. Soft-magnetic Permalloy is chosen for the nanowire material, which has been popularly used in nanowire-based study [5]–[10]. Typical magnetic parameters of Permalloy are used in the calculation for the saturation magnetization and the exchange stiffness as 8.6×10^5 A/m and 1.3×10^{-11} J/m, respectively.

There exist four different configurations of the domain walls to form a magnetic domain. It is ascribed to the different types of the domain walls, either the transverse wall or vortex wall [11], [12], and the alignment between the domain walls, either parallel or antiparallel. Fig. 2 illustrates the four configurations of (a) transverse walls with parallel polarity (TW-P), (b) transverse walls with antiparallel polarity (TW-A), (c) vortex walls with antiparallel curl (VW-A), and (d) vortex walls with parallel curl (VW-P), respectively. The gray contrast corresponds to the x component of the magnetization and the arrows indicate

Manuscript received October 09, 2008. Current version published May 20, 2009. Corresponding author: S.-B. Choe (e-mail: sugbong@snu.ac.kr).

Color versions of one or more of the figures in this paper are available online at http://ieeexplore.ieee.org.

Digital Object Identifier 10.1109/TMAG.2009.2018664

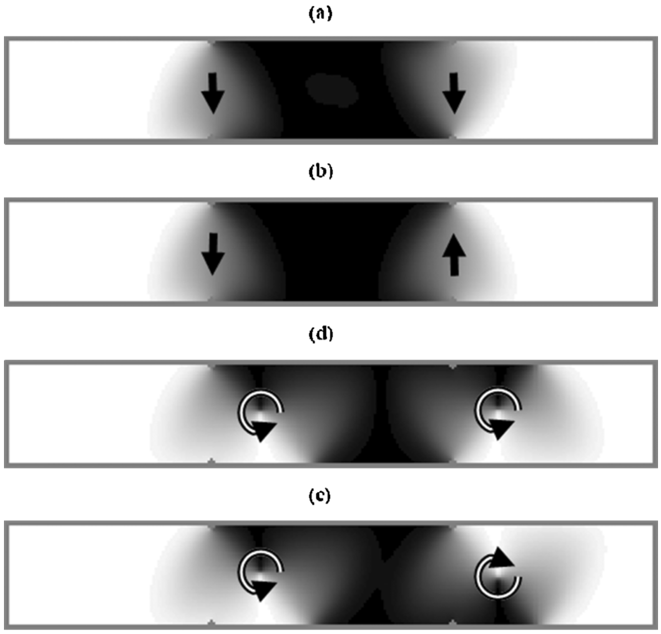

Fig. 2. Four different domain wall configurations under examination: (a) transverse walls with parallel polarity (TW-P), (b) transverse walls with antiparallel polarity (TW-A), (c) vortex walls with parallel curl (VW-P), and (d) vortex walls with antiparallel curl (VW-A).

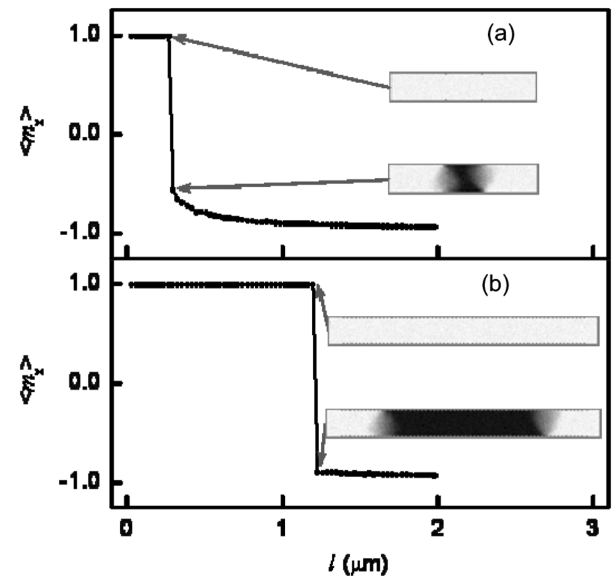

Fig. 3. Simulation results for the transverse walls with parallel polarization (TW-P). The abscissa is the length of domains initially placed and the ordinate is the average of the x-component of the magnetization over the area of the initial domain.

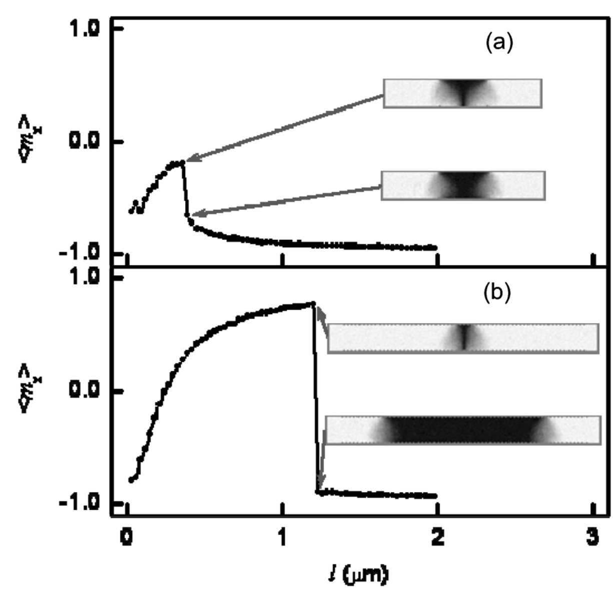

Fig. 4. Simulation results for the transverse walls with antiparallel polarization (TW-A). The abscissa is the length of domains initially placed and the ordinate is the average of the x-component of the magnetization over the area of the initial domain.

the magnetization direction inside the domain walls. A magnetic domain with the length l is initially placed with each domain-wall configuration and then, the stability is examined by checking whether the magnetic domain is collapsed or not. The micromagnetic calculation is performed by OOMMF [13] with the finite temperature module [14]. The cell size is chosen to be 5 nm, slightly smaller than the exchange length ($\sim$5.3 nm). The effect from the cell size is found to be about a few % in comparison with the results with a smaller cell size (2.5 nm). The Gilbert damping parameter is 0.02 as typical in Permalloy and the simulation time step is fixed to 2.5×10^{-14} s for the Langevin stochastic fluctuation. The stability of the magnetic domains is tested by carrying out the simulation up to 1×10^{-7} s. All the simulation results presented here are obtained at 300 K.

III. Results and Discussion

The stability of the magnetic domains is found to be sensitive to the domain wall types and the pinning structure, but insensitive to the domain wall alignment. In Fig. 3, we plot the final magnetization state of the 200-nm-wide nanowires with respect to l for the TW-P configuration of (a) the case I and (b) the case II, respectively. The ordinate is scaled with $\langle m_\mathrm{x} \rangle$, which is the average value of the x component of the magnetization at the final state. The average is carried out over the area where the magnetic domain is initially placed. It is clearly seen from the plot that there exist a threshold—a magnetic domain smaller than the threshold is collapsed exhibiting $\langle m_\mathrm{x} \rangle = 1$, whereas a magnetic domain larger than the threshold is maintained with $\langle m_\mathrm{x} \rangle = -1$ as initially given. The images inside the figure illustrate the magnetization configuration at the final state for different l designated by the arrows.

A detailed look on the magnetization process reveals that there exists an attractive force between the domain walls via the magnetostatic interaction. The magnetic domain is collapsed when the interaction force is larger than the domain-wall pinning force, which is produced by the vacancy at the sample edge. The attractive force decreases with increasing the distance between the domain walls and thus, there exists a threshold distance where the attractive force equals the pinning force. Stable domains are attained for lengths larger than the threshold and thus, we denote the threshold as the stable domain length l_S.

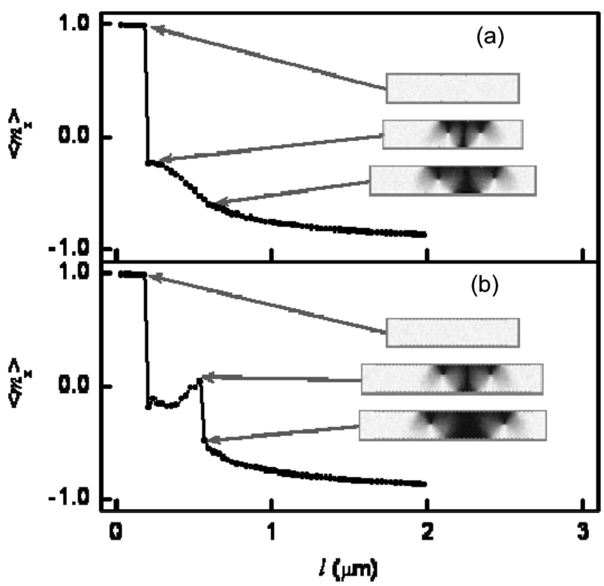

Fig. 5. Simulation results for the vortex walls with parallel polarization (VW-P). The abscissa is the length of domains initially placed and the ordinate is the average of the x-component of the magnetization over the area of the initial domain.

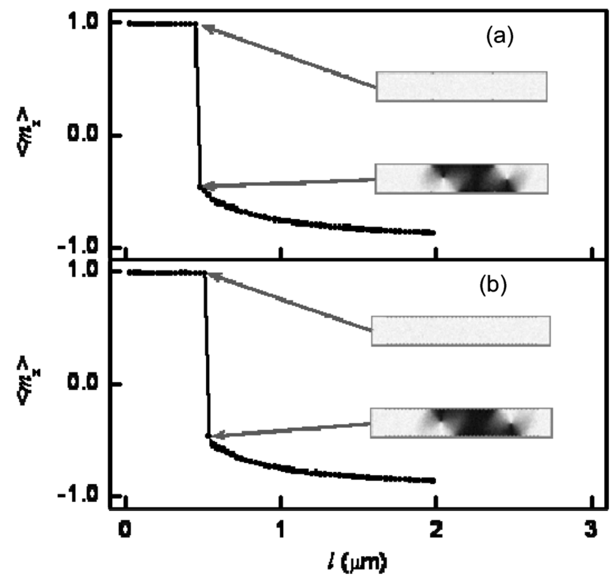

Fig. 6. Simulation results for the vortex walls with antiparallel polarization (VW-A). The abscissa is the length of domains initially placed and the ordinate is the average of the x-component of the magnetization over the area of the initial domain.

A similar behavior is observed for the case of the opposite alignment of the domain walls. Fig. 4 shows the results for the TW-A configuration. It is again observed that the attractive force between the domain walls triggers the deformation of the domain structure. However, it is interesting to note that the domain walls do not annihilate but create a 360° domain-wall structure [15], which is distinct from the vortex domain wall. The 360° domain-wall structure is observed for all the wire width under examination from 60 to 200 nm. It is found to be quite robust against to the thermal fluctuation, but easily removed by applying a small magnetic field.

It is interesting to note that the stable domain length is very sensitive to the wire edge profile. The stable domain length of the case I is predicted to be 0.27 μm and 0.36 μm for the TW-P and TW-A configurations, respectively, whereas the stable domain length of the case II is 1.2 μm for both the TW-P and TW-A configurations. Note that even though the same vacant cells in the simulation are used for both the edge roughness and the notches at which the domain walls are initially placed, the pinning force is sensitively dependent on the neighboring wire edge profile. It is because the edge roughness deforms the pinning potential profile and consequently, reduces the pinning strength of the notches. The domain walls in the case II are, therefore, pinned by a smaller pinning strength than those in the case I and consequently, the case II exhibits larger l_S than the case I.

On the other hand, for the vortex walls, the stable domain length is found to be insensitive to the pinning structure as seen in Fig. 5 for the VW-P configuration and Fig. 6 for the VW-A configuration, respectively. It can be understood by considering the flux closure structure of the vortex walls. Due to the flux closure structure, the magnetostatic interaction between the vortex walls is very limited to a short range. A sufficiently large attractive force is therefore attained only when the domain walls are close enough, at the vicinity of the direct overlap between the closest borders of the domain walls. The threshold length is thus given to be a little bit larger than the finite size of the vortex walls, which is insensitive to the pinning strength of the notches.

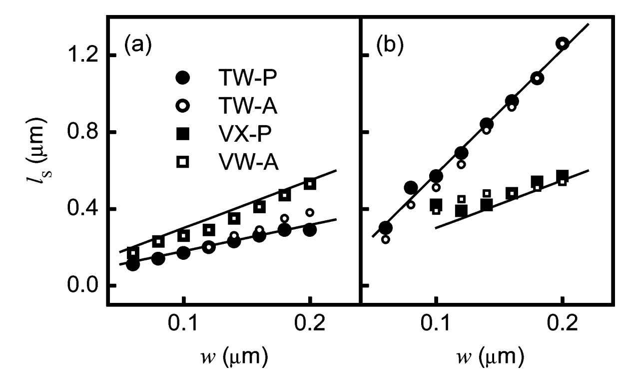

Fig. 7. The stable domain length l_S with respect to the wire width w for (a) the case I and (b) the case II, respectively. Four different domain wall configurations are shown by different symbols as denoted in the figure.

Despite of abrupt annihilation of the domain walls in the VW-A configuration, the domain walls in the VW-P configuration are merged to form 360° domain walls as shown in Fig. 5, as like as the TW-A configuration. This merged domain walls are also robust against to the thermal fluctuation, but collapsed under a small magnetic field.

The stable domain lengths are summarized in Fig. 7. The figure shows l_S with respect to w for (a) the case I and (b) the case II, respectively. The four domain-wall configurations are shown by different symbols as denoted in the figure. The solid lines are guide to the eyes with the best linear fit to each domain-wall configuration. The scattered dots are ascribed to the stochasticity of the finite temperature. The fitting parameters for the best fit are $l_S = 0.04 + 1.4\,w$ and $l_S = -0.07 + 6.5\,w$ for the transverse walls of the case I and II, respectively, and

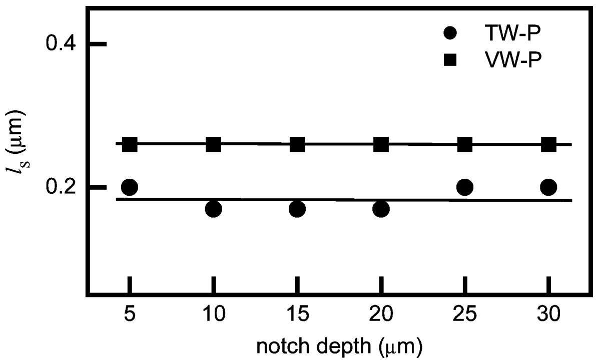

Fig. 8. The stable domain length l_S with respect to the notch depth for 100-nm-wide nanowire for the case I.

$l_S = 0.05 + 2.5\,w$ for the vortex walls of both the case I and II. It is clear from the figure that the stable domain length is very sensitive to the domain wall type—either transverse wall or vortex wall, but insensitive to the domain wall alignment. In addition, the stable domain length with the transverse domain walls is much influenced by the wire edge profile—with or without edge roughness, whereas the domains with the vortex domain walls are almost independent to the wire edge profile. Thus, one can conclude that the control of the domain wall type is practically of importance in determining the minimum stable domain size for high density data storage, and the vortex walls have an advantage of the regular stable domain size irrespective to the wire edge profile.

Finally, we test the effect of the notch depth. Fig. 8 exhibits the stable domain lengths with respect to the notch depth, for the case I of 100-nm-wide nanowire. As clearly seen from the figure, the stable domain length is insensitive to the notch depth. It is ascribed to the fact that for the case I, the collapse of the domains is triggered by direct overlapping of the domain walls and thus, the stable domain length is solely determined by the finite size of the domain wall width, which is less sensitive to the notch depth.

IV. Conclusion

The stability of the magnetic domains in ferromagnetic Permalloy nanowires is examined by micromagnetic prediction with thermal fluctuation. The size of the stable magnetic domains is found to be sensitive to the domain wall types, but insensitive to the domain wall alignment. The domains with the vortex walls provide regular stable domains irrespective to the wire edge roughness, giving the stable domain length to be about 2.5 times the wire width.

Acknowledgment

This study was supported by the KOSEF through the NRL program (R0A-2007-000-20032-0).

References

[1] L. Thomas, M. Hayashi, X. Jiang, R. Moriya, C. Rettner, and S. S. P. Parkin, "Oscillatory dependence of current-driven magnetic domain wall motion on current pulse length," *Nature*, vol. 443, no. 7108, pp. 197–200, Sept. 2006.

[2] D. A. Allwood, G. Xiong, C. C. Faulkner, D. Atkinson, D. Petit, and R. P. Cowburn, "Magnetic domain-wall logic," *Science*, vol. 309, no. 5741, pp. 1688–1692, Sept. 2005.

[3] S.-B. Choe, "Spin reorientation transition of ferromagnetic nanowires with perpendicular magnetic anisotropy," *Appl. Phys. Lett.*, vol. 92, no. 6, p. 062506, Feb. 2008.

[4] E. Martinez, L. Lopez-Diaz, O. Alejos, L. Torres, and C. Tristan, "Thermal effects on domainwall depinning from a single notch," *Phys. Rev. Lett.*, vol. 98, no. 26, p. 267202, June 2007.

[5] M. Kläui, C. A. F. Vaz, J. Rothman, J. A. C. Bland, W. Wernsdorfer, G. Faini, and E. Cambril, "DomainWall pinning in narrow ferromagnetic ring structures probed by magnetoresistance measurements," *Phys. Rev. Lett.*, vol. 90, no. 9, p. 097202, Mar. 2003.

[6] M. Hayashi, L. Thomas, C. Rettner, R. Moriya, X. Jiang, and S. S. P. Parkin, "Dependence of current and field driven depinning of domain-walls on their structure and chirality in permalloy nanowires," *Phys. Rev. Lett.*, vol. 97, no. 20, p. 207205, Nov. 2006.

[7] C. K. Lim, T. Devolder, C. Chappert, J. Grollier, V. Cros, A. Vaurès, A. Fert, and G. Faini, "Domain wall displacement induced by sub-nanosecond pulsed current," *Appl. Phys. Lett.*, vol. 84, no. 15, p. 2820, Feb. 2004.

[8] M. Tsoi, R. E. Fontana, and S. S. P. Parkin, "Magnetic domain wall motion triggered by an electric current," *Appl. Phys. Lett.*, vol. 83, no. 13, p. 2617, Mar. 2003.

[9] M. Hayashi, L. Thomas, Y. B. Bazaliy, C. Rettner, R. Moriya, X. Jiang, and S. S. P. Parkin, "Influence of current on field-driven domainwall motion in permalloy nanowires from time resolved measurements of anisotropic magnetoresistance," *Phys. Rev. Lett.*, vol. 96, no. 19, p. 197207, May 2006.

[10] K.-J. Kim, J.-C. Lee, S.-B. Choe, and K.-H. Shin, "Joule heating in ferromagnetic nanowires: Prediction and observation," *Appl. Phys. Lett.*, vol. 92, no. 19, p. 192509, May 2008.

[11] R. D. McMichael and M. J. Donahue, "Head to head domain wall structures in thin magnetic strips," *IEEE Trans. Magn.*, vol. 33, no. 5, pp. 4167–4169, Sept. 1997.

[12] M. Kläui, C. A. F. Vaz, J. A. C. Bland, and L. J. Heyderman, "Head-to-head domain-wall phase diagram in mesoscopic ring magnets," *Appl. Phys. Lett.*, vol. 85, no. 23, pp. 5637–5639, Dec. 2004.

[13] M. Donahue and D. Porter, OOMMF Oct. 30, 2000 [Online]. Available: http://math.nist.gov/oommf/, (1.2a3 ver.)[Online]. Available

[14] O. Lemcke, UHH_ThetaEvolve Feb. 6, 2004 [Online]. Available: http://www.nanoscience.de/group_r/stm-spstm/projects/temperature/download.shtml, [Online]. Available

[15] A. Kubetzka, O. Pietzsch, M. Bode, and R. Wiesendanger, "Spin-polarized scanning tunneling microscopy study of 360° walls in an external magnetic field," *Phys. Rev. B*, vol. 67, no. 2, p. 020401(R), Jan. 2003.